Dynamic Analysis of Dark–Light Changes of the Anterior Chamber Angle with Anterior Segment OCT

Christopher Kai-shun Leung,[1,2,3] *Carol Yim Lui Cheung,*[1,3] *Haitao Li,*[1] *Syril Dorairaj,*[4] *Cedric Ka Fai Yiu,*[5] *Amy Lee Wong,*[1] *Jeffrey Liebmann,*[4,6] *Robert Ritch,*[4,6] *Robert Weinreb,*[2] *and Dennis Shun Chiu Lam*[1]

Purpose. To describe the use of anterior segment optical coherence tomography (OCT) in studying the dynamic dark–light changes of the anterior chamber angle.

Methods. Thirty-seven normal subjects with open angles on dark-room gonioscopy and 18 subjects with narrow angles were analyzed. The dynamic dark–light changes of the anterior-chamber angle were captured with real-time video recording. The angle opening distance (AOD500) and trabecular iris space area (TISA500) of the nasal angle and the pupil diameter in each of the representative serial images were measured. Linear regression analysis was performed to investigate the association between AOD500/TISA500 and pupil diameter. Demographic and biometry measurements associated with the AOD difference ($AOD500_{(light)} - AOD500_{(dark)}$) and TISA difference ($TISA500_{(light)} - TISA500_{(dark)}$) were analyzed with univariate and multivariate regression models.

Results. The AOD500/TISA500 measured in the light in the open-angle and the narrow-angle groups were 694 ± 330 μm/0.24 ± 0.10 mm^2 and 265 ± 78 μm/0.10 ± 0.03 mm^2, respectively. These values were significantly greater than the AOD500/TISA500 measured in the dark (492 ± 265 μm/0.16 ± 0.08 mm^2 and 119 ± 82 μm/0.05 ± 0.04 mm^2, respectively, all with $P < 0.001$). The ranges of the AOD/TISA difference were 13 to 817μm/0.011 to 0.154 mm^2, with an average of 180 μm/0.073 mm^2. Multivariate regression analysis identified a positive correlation between anterior chamber depth and the AOD/TISA difference. Fifty eyes showed significant correlations between AOD/TISA and pupil diameter, whereas one eye showed no association. Four eyes in the narrow angle group developed appositional angle closure in the dark.

Conclusions. The dynamic dark–light changes of the anterior chamber angle can be imaged and analyzed with anterior segment OCT. Although the angle width generally decreased linearly with increasing pupil diameter, the differences of the angle width measured in the dark and in the light varied substantially among individuals. (*Invest Ophthalmol Vis Sci.* 2007;48:4116–4122) DOI:10.1167/iovs.07-0010

Primary angle closure is the leading cause of glaucoma-induced blindness in the East Asian population.[1] Evaluation of the width of the anterior chamber angle and its inlet during the ophthalmic examination is essential in determining the susceptibility of the angle to closure. The gold standard for examining the anterior chamber angle has been indentation gonioscopy. The interpretation of gonioscopic findings, however, is subjective and only semiquantitative. Most important, angle structures visible during gonioscopy vary, depending on the lighting condition and the amount of indentation on the cornea. When assessing a patient with a narrow angle for occludability, it is important to perform gonioscopy in a completely darkened room, using the smallest square of light for a slit beam set off the pupil, so as to avoid stimulating the pupillary light reflex and with no indentation on the cornea. However, one cannot be totally certain that slit lamp illumination has no effect on the angle appearance, and there is no way to confirm the complete absence of indentation during gonioscopy. While illumination can cause miosis and lead to widening of the angle, any forces exerted on the corneal surface during the direct contact of the gonioscopy lens could translate to the aqueous humor in the anterior chamber, with subsequent changes in the angle configuration. True measurement of angle width, independent of the effects of illumination and indentation on the cornea, is difficult, if not impossible to obtain with gonioscopy.

The Visante anterior segment optical coherence tomograph (Carl Zeiss Meditec, Inc. Dublin, CA) was recently introduced to provide noncontact and noninvasive optical imaging of the anterior segment. With this technology, detailed spatial relationships of the structures forming the anterior chamber angle can be visualized and objective angle measurements performed. In addition, the use of the infrared laser and the noncontact technique during examination permits capture of angle morphology in the dark. Anterior segment OCT thus has the potential to provide valuable quantitative and spatial information regarding dynamic changes of the angle configuration not provided by standard gonioscopy. In this study, we investigated and measured the dark–light dynamic changes of the anterior chamber angle with real-time video capture using the anterior segment OCT.

Materials and Methods

The study was conducted in accordance with the ethical standards stated in the 1964 Declaration of Helsinki and approved by the local

From the [1]Department of Ophthalmology and Visual Sciences, The Chinese University of Hong Kong, Hong Kong, Peoples Republic of China; the [2]Hamilton Glaucoma Center, University of California, San Diego, California; [4]The New York Eye and Ear Infirmary, New York, New York; the [5]Department of Applied Mathematics, Hong Kong Polytechnic University, Hong Kong, Peoples Republic of China; and the [6]New York Medical College, Valhalla, New York.

[3]Contributed equally to the work and therefore should be considered equivalent authors.

RW received research support in the form of instruments from and is a consultant for Carl Zeiss Meditec, Inc. CKSL has received an honorarium from Carl Zeiss Meditec, Inc. for a conference presentation.

Submitted for publication January 4, 2007; revised March 30, April 22 and 25, and May 27, 2007; accepted July 6, 2007.

Disclosure: **C.K.-s. Leung**, Carl Zeiss Meditec, Inc. (R); **C.Y.L. Cheung**, None; **H. Li**, None; **S. Dorairaj**, None; **C.K.F. Yiu**, None; **A.L. Wong**, None; **J. Liebmann**, None;**R. Ritch**, None; **R. Weinreb**, Carl Zeiss Meditec, Inc. (C, F); **D.S.C. Lam**, None

The publication costs of this article were defrayed in part by page charge payment. This article must therefore be marked "*advertisement*" in accordance with 18 U.S.C. §1734 solely to indicate this fact.

Corresponding author: Christopher Kai-shun Leung, Department of Ophthalmology and Visual Sciences, The Chinese University of Hong Kong, University Eye Center, Hong Kong Eye Hospital, 147K Argyle Street, Hong Kong; tlims00@hotmail.com.

TABLE 1. Comparisons of Demographic Data and Angle Width Measurements between Open- and Narrow-Angle Groups

	Open Angle (Mean ± SD) $n = 37$	Narrow Angle (Mean ± SD) $n = 18$	P*
Age (y)	53.5 ± 19.6	69.6 ± 7.7	0.002
Gender (male/female)	23/14	6/12	0.085†
Spherical equivalent (D)	−1.45 ± 2.80	0.37 ± 2.16	0.021
Anterior chamber depth (mm)	3.25 ± 0.50	2.43 ± 0.25	<0.001
Axial length (mm)	24.38 ± 1.23	22.92 ± 0.81	<0.001
Dark-room gonioscopy grading (Shaffer)	3.41 ± 0.50	1.44 ± 0.51	<0.001‡
AOD $500_{(dark)}$ (μm)	492 ± 265	119 ± 82	<0.001
AOD $500_{(light)}$ (μm)	694 ± 330	265 ± 78	<0.001
TISA $500_{(dark)}$ (mm^2)	0.16 ± 0.08	0.05 ± 0.04	<0.001
TISA $500_{(light)}$ (mm^2)	0.24 ± 0.10	0.10 ± 0.03	<0.001

* Independent *t*-test.
† χ^2 test.
‡ Mann-Whitney test.

Clinical Research Ethics Committee. Informed consent was obtained from 55 Chinese patients, followed up in the Department of Ophthalmology, Hong Kong Eye Hospital, after explanation of the purpose and nature of the investigation. All subjects underwent a complete ophthalmic examination including visual acuity with refraction, A-scan ultrasound biometry, slit lamp biomicroscopy, intraocular pressure measurement, and fundus examination. Gonioscopy was performed to examine each quadrant of the anterior chamber angle using a Goldmann two-mirror lens with a short and narrow beam width in a darkened room. Caution was exercised to avoid having the slit beam light fall on the pupil. The Shaffer classification system was used to grade the angles.[2] An open angle was defined as having a Shaffer grade greater than 2 during dark-room gonioscopy, whereas a narrow angle was defined as having a Shaffer grade 2 or less. Since the objective of this study was to describe the dynamic dark–light changes of the anterior chamber angle, we selected only the nasal angle for analysis. During the recruitment period from March to June 2006, 37 subjects with open angles and 18 with narrow angles agreed to participate. Subjects with evidence of peripheral anterior synechiae on indentation, plateau iris configuration, history of use of any topical or systemic medication that could affect the drainage angle or pupillary reflex and history of any previous intraocular surgery, laser trabeculoplasty, laser iridotomy, laser iridoplasty, or trauma were excluded from the study. When both eyes of the same patient were eligible, one eye was randomly selected for inclusion in the study.

Visante Anterior Segment Optical Coherence Tomography Imaging

Each selected eye was imaged with anterior segment optical coherence tomography (The Zeiss Visante OCT Model 1000; Carl Zeiss Meditec, Dublin, CA). The Visante OCT is a noncontact, high-resolution tomographic and biomicroscopic device designed for anterior segment imaging and measurement. The imaging principle is based on low-coherence interferometry, with a 1310-nm superluminescent light-emitting diode (SLD) as the light source. Analogous to an ultrasound B-scan, the Visante OCT acquires multiple A-scans and aligns them to construct two-dimensional images. The scanning of the anterior chamber angle is a noncontact procedure during which the subject fixates on an internal fixation target (wavelength of visual aiming beam is 845 nm). The Visante OCT allows real-time imaging of the anterior chamber with scan speed of 2000 A-scans per second. The scan acquisition time is 0.125 second per line for the anterior segment single scan (limbus to limbus; eight frames per second). To capture the dynamic change of the angle configuration in response to dark–light changes, video recording software (CamStudio 2.1; Rendersoft Software; Singapore) was installed in the Visante computer with one frame recorded every 5 msec (the default recording rate). OCT imaging was performed with the protocol anterior segment single 0° to 180° (6 mm deep × 16 mm wide, with 256 A-scans per line). The scan line was manually adjusted to bisect the pupil. Video recording began once the subject had been dark adapted for about 1 minute. The room light was then turned on (light intensity measured at the subject sitting position = 368 lux). The change in pupil size, from dilation in darkness to constriction under room light, and the associated changes in angle configuration, were recorded in a video file, which was subsequently exported for editing. Each video file was reviewed with video editing software (Video Edit Magic version 4.21; Deskshare, Plainview, NY). Depending on the recording time, which varied among subjects, each video file contained 600 to 1000 images. Only the portion of images showing the smooth transition of pupil size from the dark to the light was used for the analysis. Because the video capture rate is high (the default rate is 5 msec), there were many identical images during the video capture. As we could not pinpoint where the changes occur in the image series, rather than using the approach of systematic sampling, we examined all the images to prevent skipping and missing potentially useful images showing changes in pupil size and angle configuration. Each image series was reviewed in the video editing software frame by frame, beginning from a fully dilated to a constricted pupil. Since the images were sequentially reviewed in the same viewing window, any subtle change in the images, including change in pupil size, could be detected easily by flipping the images back and forth. In other words, if there is no change in the angle configuration or pupil size, the images would appear as "static" despite changing the frames. During the video capture, any microsaccade or eye movement can be detected, both in the real-time camera and in the OCT panel, as movement of the whole eyeball, and not just the iris tip. Therefore, one can easily differentiate whether it is the movement of the iris tip or the whole eyeball. If there is microsaccade and eye tremor observed during the video capture, the capture was repeated. Since the duration for the pupil to change from a dilated to a constricted state was only a few seconds, it is not difficult for subjects to have steady fixation during this short period.

Measurement of AOD and TISA

We specifically wrote a program (in MatLab ver. 6.5; The MathWorks, Natick, MA) to measure the AOD500 and TISA500. The AOD500 was calculated as the distance from the corneal endothelium to the anterior iris surface perpendicular to a line drawn at 500 μm from the scleral spur. The TISA500 is an area bound anteriorly by the AOD500, posteriorly by a line drawn from the scleral spur perpendicular to the plane of the inner scleral wall to the opposing iris, superiorly by the inner corneoscleral wall, and inferiorly by the iris surface.[3] This parameter was used instead of the angle recess area (ARA500) because it has been proposed that the ARA may be less sensitive in identifying narrow

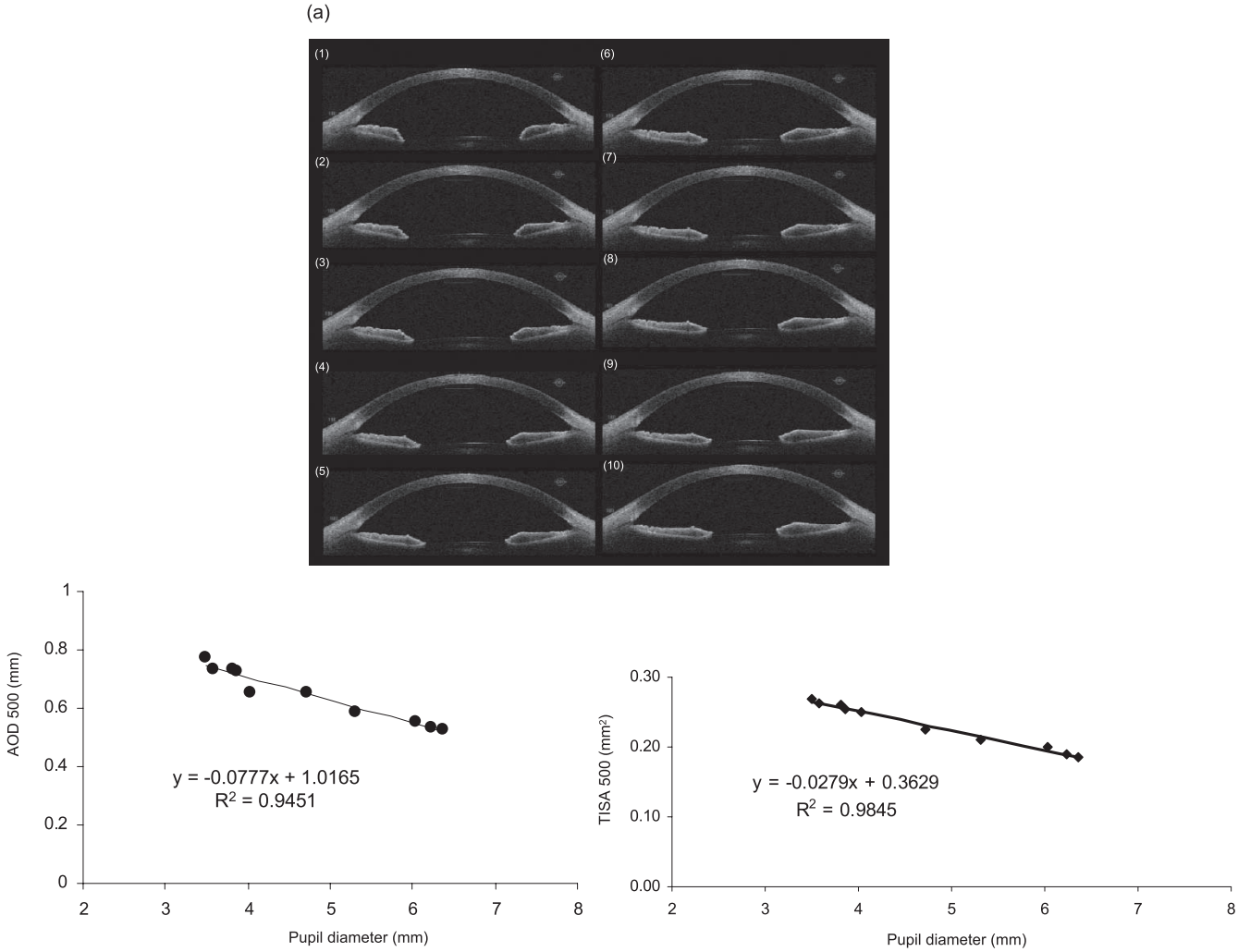

FIGURE 1. Serial anterior segment OCT images (a horizontal anterior segment single scan bisecting the pupil) captured from a real-time video recording demonstrate the changes in the anterior chamber angle configuration from dark to light (*top*). The corresponding AOD500 and TISA500 at the nasal angle and the pupil diameter in each image were measured and plotted (*bottom*). (**a**) A 66-year-old normal subject showing deceasing angle width with increasing pupil size. (**b**) An 82-year-old normal subject with angle configuration remains essentially the same, independent of the pupil size. (**c**) A 72-year-old subject with narrow angle (dark-room gonioscopy grading 1) illustrating appositional angle closure in the dark.

angles in eyes with deep angle recess.[3] The program requires the user to input the location of the scleral spur. The AOD500 and TISA500 are then calculated automatically. High repeatability (intraclass correlation [AOD500] = 0.98 [95% CI: 0.96–0.99] and intraclass correlation [TISA500] = 0.98 [95% CI: 0.96–0.99]; three measurements in a single visit) and reproducibility (intraclass correlation [AOD500] = 0.95 [95% CI: 0.90–0.97] and intraclass correlation [TISA500] = 0.94 [95% CI: 0.88–0.97]; three measurements in three separate visits) were demonstrated with the AOD500 and TISA500 measurement in a separate study in 25 subjects (Li HT et al., unpublished data, 2007).

Statistics

Statistical analysis was performed with commercial software (SPSS version 11.0; SPSS, Chicago, IL). Comparisons of the biometry parameters (axial length, spherical equivalent, axial length, and anterior chamber depth) and the AOD/TISA measurements between the open- and narrow-angle groups were performed with an independent *t*-test. The correlations between dark-room gonioscopy grading and the AOD500/TISA500 were expressed as a Spearman's rank correlation coefficient. Univariate and multivariate regression analyses were performed to determine factors (age, dark-room gonioscopy grading, spherical equivalent, axial length, and anterior chamber depth) related to the AOD difference ($AOD500_{(light)} - AOD500_{(dark)}$) and TISA difference ($TISA500_{(light)} - TISA500_{(dark)}$). Factors significant at $P < 0.05$ were included in the multiple linear regression analysis. The relationship between AOD500/TISA500 and pupil diameter in each eye was studied with linear regression analysis, and the association was expressed as a Pearson correlation coefficient.

RESULTS

Thirty-seven subjects with open angles (gonioscopy grade 3 or 4) and 18 with narrow angles (gonioscopy grade 2 or less) were imaged. The demographic data and the AOD500 and TISA500 measurements are shown in Table 1. The values of anterior chamber depth, axial length, AOD500, and TISA500 measurements were significantly smaller in the narrow-angle group (all with $P < 0.001$). The values of the AOD500 and TISA500 measured in the light were significantly higher than those measured in the dark for both open and narrow angle groups (both with $P < 0.001$). The dark-room gonioscopy grading correlated significantly with the AOD500 and TISA500 measurements in the dark (Spearman's rank correlation coefficient = 0.70 and 0.64 respectively, both with $P < 0.001$).

(b)

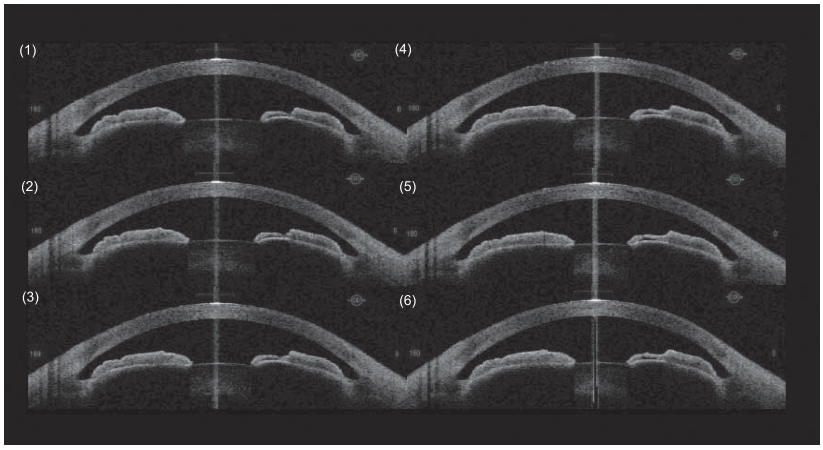

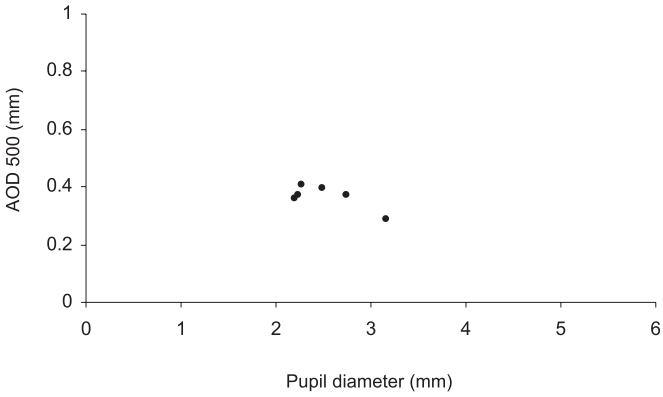

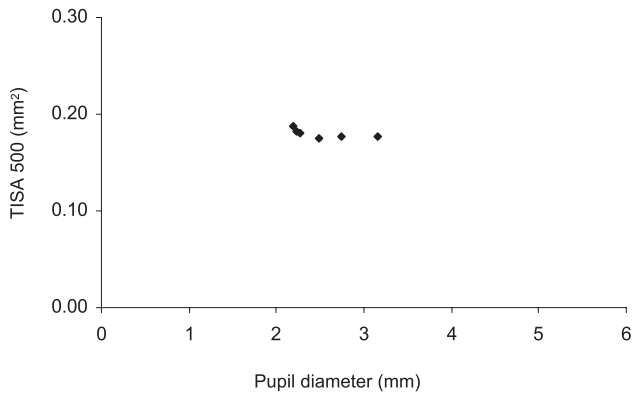

FIGURE 1. (*Continued*)

The relationship between the AOD500/TISA500 and pupil diameter in each eye was examined by linear regression analysis. The average number of images analyzed in each eye was 8.1 with range between 5 and 13 images. In 47 (85.5%) eyes, the AOD decreased linearly with increasing pupil diameter (Fig. 1a). The Pearson correlation coefficient ranged between −0.73 and −0.99 (median, −0.93). The average slope of the linear regressions of the AOD was −0.094 ± 0.042 (range: −0.040 to −0.252). TISA500 decreased linearly with increasing pupil diameter in 50 (90.9%) eyes with the Pearson correlation coefficient ranging between −0.67 and −0.99 (median, −0.93). The average slope of the linear regressions of the TISA was −0.035 ± 0.012 (range: −0.001 to −0.067). The slope of the linear regression between AOD/TISA and pupil size was higher in open angles than that in narrow angles ($P = 0.087$ for AOD; $P < 0.001$ for TISA). Only one (1.8%) eye did not show any association between AOD/TISA and pupil diameter (Fig. 1b), and four eyes (7.3%) were found to have appositional angle closure based on the AOD and TISA measurements (Fig. 1c). Of the eyes with appositional angle closure, all had a dark-room gonioscopy grade of 1. Analyses of their dynamic angle profiles revealed that the angle had been occluded before the pupil became maximally dilated in the dark (Fig. 1c).

The ranges of dark–light AOD difference ($AOD500_{(light)} - AOD500_{(dark)}$) and TISA difference ($TISA500_{(light)} - TISA500_{(dark)}$) were between 13 and 817 μm (average, 180 μm) and 0.011 to 0.154 mm^2 (average, 0.073 mm^2), respectively. Univariate regression analysis was performed to evaluate the associations between the AOD/TISA difference and age, dark-room gonioscopy grading, spherical equivalent, axial length, and anterior chamber depth, and the results are shown in Tables 2a and 3a. The AOD difference correlated with anterior chamber depth, whereas the TISA difference correlated with age and anterior chamber depth after adjustment of other factors in the multivariate regression models (Tables 2b, 3b).

DISCUSSION

Although gonioscopy is the gold standard for anterior chamber angle assessment, its inevitable need for minimal illumination to visualize the angle, the uncertainty of the change in angle configuration when a goniolens is in direct contact on the cornea, and the dependence on individual skill and experience for interpretation of the angle configuration, serve to limit its role in providing precise angle assessment. Reliable measurement of the anterior chamber angle was not possible until ultrasound biomicroscopy (UBM) became available. With UBM, detailed spatial relationships of the anterior chamber angle/iridocorneoscleral junction can be visualized and quantified. However, UBM is a close-contact immersion technique. Inadvertent corneal indentation can cause artifactitious widening of the angle.[4] By the time the image is captured, it may be difficult to judge the exact globe position and the precise clock-hour location at which the scan was aligned. As a result, intra- and interobserver reproducibilities for angle measurements have

(c)

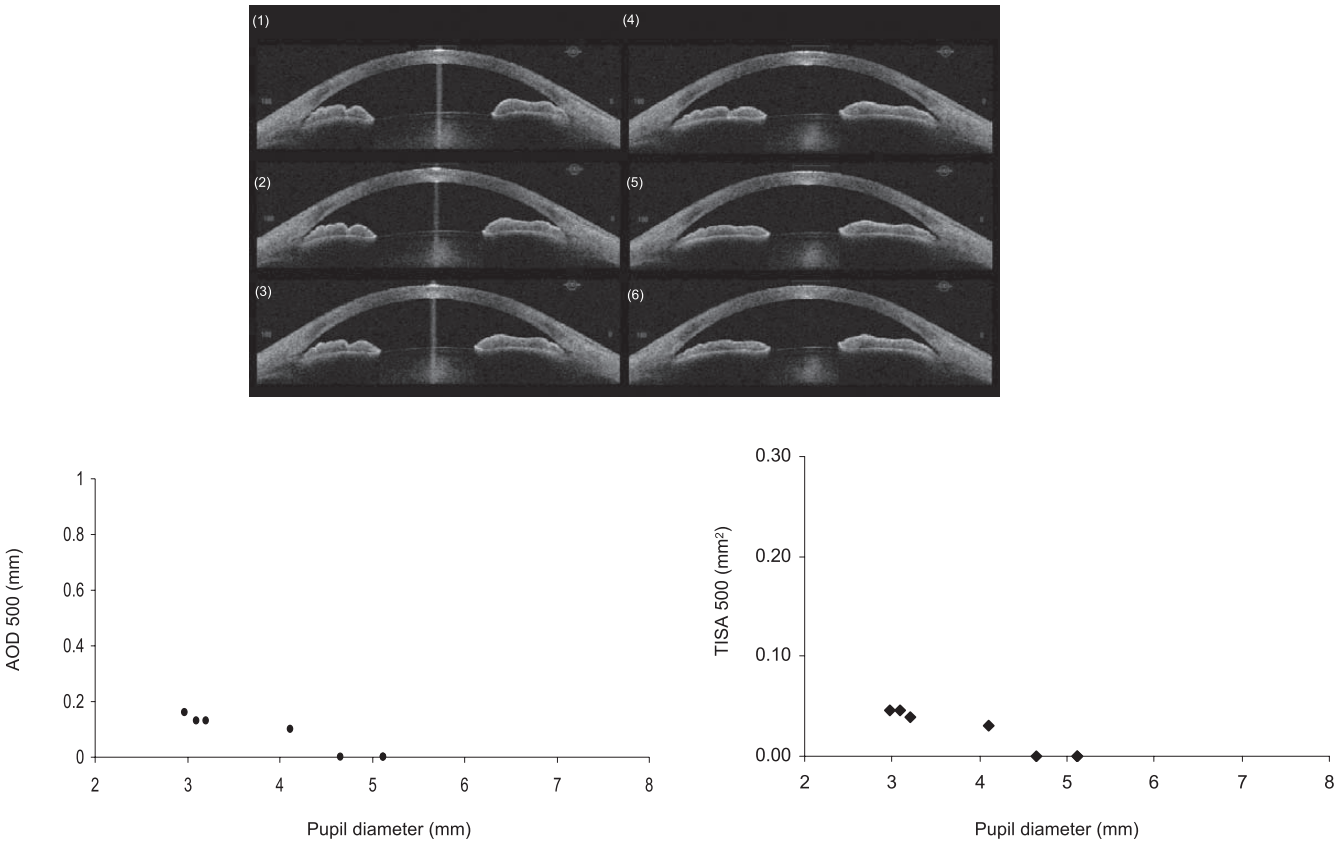

FIGURE 1. (*Continued*)

been generally poor.[5,6] The Visante anterior segment OCT, in contrast, is a noncontact imaging technology with image resolution higher than that of UBM (axial resolution of 18 μm in Visante OCT versus 50 μm in UBM). The ability to visualize the scan position in the real-time camera panel and the fast scan speed allow for a unique opportunity to study the dynamic dark–light changes of the anterior chamber angle configuration precisely.

TABLE 2. Univariate and Multivariate Regressions for AOD

a. Correlations between the Difference of AOD (AOD $500_{(light)}$ − AOD $500_{(dark)}$) and Subject Parameters

	*r**	*P*
Age (y)	−0.415	0.002
Dark-room gonioscopy grading (Shaffer)	0.215	0.115
Spherical equivalent (D)	−0.117	0.394
Axial length (mm)	0.205	0.134
Anterior chamber depth (mm)	0.463	<0.001

* *r* is expressed as the Pearson correlation coefficient for age, spherical equivalent, axial length and anterior chamber depth, and as the Spearman rank correlation coefficient for dark room gonioscopy grading (Shaffer).

b. Multivariate Regression Model with the AOD Difference (AOD $500_{(light)}$ − AOD $500_{(dark)}$) as a Dependent Variable and Subject Parameters as Predictors

	Standardized Coefficients (β)	*P*
Age (y)	−0.201	0.206
Anterior chamber depth (mm)	0.335	0.038

$r^2 = 0.488$; $P < 0.001$.

TABLE 3. Univariate and Multivariate Regressions for TISA

a. Correlations between the Difference of TISA (TISA $500_{(light)}$ − TISA $500_{(dark)}$) and the Subject Parameters

	*r**	*P*
Age (y)	−0.585	<0.001
Dark-room gonioscopy grading (Shaffer)	0.409	0.002
Spherical equivalent (D)	−0.236	0.083
Axial length (mm)	0.389	0.003
Anterior chamber depth (mm)	0.669	<0.001

* *r* is expressed as the Pearson correlation coefficient for age, spherical equivalent, axial length and anterior chamber depth, and as the Spearman rank correlation coefficient for dark room gonioscopy grading (Shaffer).

b. Multivariate Regression Model with the TISA Difference (TISA $500_{(light)}$ − TISA $500_{(dark)}$) as a Dependent Variable and the Subject Parameters as Predictors

	Standardized Coefficients (β)	*P*
Age (y)	−0.339	0.013
Dark-room gonioscopy grading (Shaffer)	−0.202	0.164
Axial length (mm)	−0.196	0.168
Anterior chamber depth (mm)	0.735	<0.001

$r^2 = 0.531$; $P < 0.001$.

The differences in anterior chamber angle measurements both in light and dark conditions have been previously investigated with UBM. Woo et al.[7] found the AOD500 to be significantly greater in the light than in the dark, with a mean difference of 89 μm in 24 patients with pupillary block. UBM has also been recommended for provocative testing to determine whether an angle is occludable, as appositional closure was more frequently detected in the dark.[8] With the use of the Visante OCT, our results are in agreement with previous UBM studies. The AOD500 and TISA500 in the light were significantly greater than that in the dark. Given the observation that the range of the AOD/TISA difference ($AOD500/TISA500_{(light)} - AOD500/TISA500_{(dark)}$) were large (13–817 μm for AOD; 0.011–0.154 mm^2 for TISA), it is conceivable that the corresponding discrepancy in gonioscopy grading could also vary considerably. In some cases, gonioscopy assessment could be minimally affected by dark–light changes, whereas in others, the grading could change substantially (up to an AOD/TISA difference of 817 μm/0.154 mm^2) depending on the effect of background illumination on the pupil size. In most population studies on glaucoma prevalence, gonioscopy was performed at a low level of ambient illumination for practical reasons[9–11] although dark-room gonioscopy was performed in some other studies.[12,13] Our results demonstrate the importance of standardizing the background light intensity in the evaluation of anterior chamber angle configuration. The effect of ambient–slit lamp illumination on the pupil size could be influential in the determination of the angle width and its measurement. Multivariate regression analysis indicated that deeper anterior chamber depth was significantly associated with a larger difference in the AOD ($AOD500_{(light)} - AOD500_{(dark)}$) and TISA ($TISA500_{(light)} - TISA500_{(dark)}$). Although a shallow anterior chamber is a risk factor for development of angle closure, caution should also be exercised when performing gonioscopy in subjects with normal or deep anterior chambers, because more variation in the assessment of angle width would be expected.

Different patterns (Fig. 1) were observed in the dynamic profile describing the relationship between AOD500/TISA500 and pupil size. The AOD500 and TISA500 decreased linearly (median Pearson correlation coefficient = −0.93 for both AOD500 and TISA500) with increasing pupil size in most cases. It is estimated that for each millimeter change in pupil size, there is an average of a 94-μm change in the AOD500 and 0.035 mm^2 change in the TISA500. In contrast, the AOD and TISA remained essentially constant and independent of pupil size in an eye with relatively deep angle recess (Fig. 1b). Dim light is one of the precipitating factors in acute angle closure. With the dynamic analysis of the anterior chamber angle profiles, we showed that appositional closure could occur before the pupil was maximally dilated in the dark (Fig. 1c). One of the characteristic signs associated with acute angle closure is a "mid-dilated" pupil. The dark–light dynamic capture illustrates that appositional angle closure could be developed in an eye with a mid-dilated pupil.

We found that the slope of the linear regression between AOD/TISA and pupil size was higher in eyes with open angles than in those with narrow angles. In other words, for each millimeter increase in pupil size, the angle width decreased more in the eyes with open angles than in those with narrow angles. This interesting finding suggests that the iris is probably more "dynamic" in eyes with open angles than in narrow angles. Appositional closure likely occurs in eyes with short initial iridocorneal distance.

Because the objective of this study was to describe the dynamic dark–light changes of the anterior chamber angle with a new technology, we focused only on the nasal angle for analysis. Although no significant difference in AOD among superior, nasal, inferior and temporal quadrants, in either the light or the dark, was found in a previous UBM study,[7] it is possible that different patterns of angle dynamics in response to dark–light changes may be found in different quadrants. Of note, scanning the superior and inferior angles with the Visante OCT could be difficult because manipulation of eyelids would be required to expose the limbus for the imaging. With the use of a signal source of a super luminescent diode (SLD) with a wavelength of 1310 nm, it was not possible to investigate the dynamic changes of the ciliary body position in relation to the angle with the Visante OCT. Nevertheless, the Visante OCT was able to provide high-quality images of the angle width. Although it is mentioned in the operating manual that the wavelength of the visual aiming beam is 845 nm, there are no data available in the literature or from the company that indicate to what extent the luminance of the internal fixation light affects pupillary response. It is uncertain whether images captured in the dark by the anterior segment OCT could reflect the "true" pupillary response in darkness.

It is yet to be investigated whether the angle configuration continues to change after the pupil becomes constricted. Continued aqueous humor formation will inflate the posterior chamber until the pressure difference between the anterior chamber and the posterior chamber is in equilibrium with the resistance to flow in the channel between the iris near the pupil and the lens.

Instead of standardizing the pupil size with adjustment of different light intensity, the use of the current video capture technique allows a rapid assessment of the angle dynamics. However, images available for analysis were limited by the scan speed of the instrument and the speed of individual pupillary response. In this study, the average number of images available for analysis in each eye was 8.1 (range: 5–13 images). Although this information may not be adequate to describe nonlinear relationships, the high values of the correlation coefficient in most eyes in our series suggested that the AOD/TISA decreased in essentially a linear fashion with increasing pupil size. Because the selection of images for analysis were based on the changes of angle or iris configuration observed in the captured image series, it may have been difficult to detect iris motion when there was subtle eye movement. Nevertheless, video capture would have been repeated if a microsaccade and eye tremor had been observed. Because of the scan geometry of the scan probe and the refraction at smooth surfaces of the eye, a built-in dewarping algorithm is incorporated in the Visante OCT to correct for image misalignment. This correction, however, was not available when images were directly analyzed from video capture. Precise measurement of the anatomic changes requires removal of the optical distortion, and it is unknown how much the dewarping influences the angle measurement. Nevertheless, we believe the impact would be minimal in the study of the relationship between AOD/TISA and pupil size.

In summary, the anterior segment OCT can provide a noncontact approach to analyze the dynamic dark–light changes of the anterior chamber angle. Our results demonstrate the impact of lighting conditions during anterior chamber angle assessment and the different patterns of dynamic profile of the anterior chamber angle. Studying the dark–light dynamic profile of the angle may provide a more comprehensive assessment of individual risks of development of primary-angle closure and may enhance our understanding of the pathophysiology involved in different types of angle closure glaucoma.

References

1. Foster PJ, Johnson GJ. Glaucoma in China: how big is the problem? *Br J Ophthalmol*. 2001;85:1277–1282.
2. Shaffer RN. A suggested anatomic classification to define the pupillary block glaucomas. *Invest Ophthalmol*. 1973;12:540–542.
3. Radhakrishnan S, Goldsmith J, Huang D, et al. Comparison of optical coherence tomography and ultrasound biomicroscopy for detection of narrow anterior chamber angles. *Arch Ophthalmol*. 2005;123(8):1053–1059.
4. Ishikawa H, Inazumi K, Liebmann JM, et al. Inadvertent corneal indentation can cause artifactitious widening of the iridocorneal angle on ultrasound biomicroscopy. *Ophthalmic Surg Lasers*. 2000;31:342–345.
5. Tello C, Liebmann J, Potash SD, et al. Measurement of ultrasound biomicroscopy images: intraobserver and interobserver reliability. *Invest Ophthalmol Vis Sci*. 1994;35:3549–3552.
6. Urbak SF, Pedersen JK, Thorsen TT. Ultrasound biomicroscopy. II. Intraobserver and interobserver reproducibility of measurements. *Acta Ophthalmol Scand*. 1998;76:546–549.
7. Woo EK, Pavlin CJ, Slomovic A, et al. Ultrasound biomicroscopic quantitative analysis of light-dark changes associated with pupillary block. *Am J Ophthalmol*. 1999;127:43–47.
8. Ishikawa H, Esaki K, Liebmann JM, et al. Ultrasound biomicroscopy dark room provocative testing: a quantitative method for estimating anterior chamber angle width. *Jpn J Ophthalmol*. 1999;43:526–534.
9. He M, Foster PJ, Ge J, et al. Prevalence and clinical characteristics of glaucoma in adult Chinese: a population-based study in Liwan District, Guangzhou. *Invest Ophthalmol Vis Sci*. 2006;47:2782–2788.
10. Vijaya L, George R, Arvind H, et al. Prevalence of angle-closure disease in a rural southern Indian population. *Arch Ophthalmol*. 2006;124:403–409.
11. Foster PJ, Machin D, Wong TY, et al. Determinants of intraocular pressure and its association with glaucomatous optic neuropathy in Chinese Singaporeans: the Tanjong Pagar Study. *Invest Ophthalmol Vis Sci*. 2003;44:3885–3891.
12. Yamamoto T, Iwase A, Araie M, et al. The Tajimi Study report 2: prevalence of primary angle closure and secondary glaucoma in a Japanese population. *Ophthalmology*. 2005;112:1661–1669.
13. Wirbelauer C, Karandish A, Haberle H, et al. Noncontact goniometry with optical coherence tomography. *Arch Ophthalmol*. 2005;123:179–185.